Available online at www.sciencedirect.com
SCIENCE DIRECT®
ELSEVIER
Sensors and Actuators A 120 (2005) 249–256
SENSORS AND ACTUATORS A PHYSICAL
www.elsevier.com/locate/sna

Study of a 2 × 2 MOEMS optical switch with electrostatic actuating

Dong-Ming Sun[a], Wei Dong[a,b], Guo-Dong Wang[a], Cai-Xia Liu[a], Xin Yan[a], Bao-Kun Xu[a], Wei-You Chen[a,*]

[a] *College of Electronic Science and Engineering, State Key Laboratory on Integrated Optoelectronics, Jilin University, Changchun 130023, China*
[b] *Changchun Institute of Optics, Fine Mechanics and Physics, Chinese Academy of Sciences, Changchun 130021, China*

Received 17 September 2004; received in revised form 15 November 2004; accepted 28 November 2004
Available online 7 January 2005

Abstract

Based on the torsion dynamic theory, the method and relative formulae are presented for analyzing the actuating voltage and the switching time, on which the effect of the air squeeze film damping is already considered, for a 2 × 2 MOEMS optical switch with electrostatic actuating. The computed results show that the switching time will increase markedly under considering the air damping. Furthermore, an optical technique is described for the measurement of the actuating voltage and switching time of the device. Theoretical and experimental results obtained demonstrate the feasibility of the proposed method. The actuating voltage is about 50 V, and the switching time $T_{\rm off}$ and $T_{\rm on}$ are about 4.8 and 12.5 ms, respectively.
© 2004 Elsevier B.V. All rights reserved.

Keywords: MOEMS; Electrostatic actuating; Air squeeze film damping; Linear array CCD; Optical switch

1. Introduction

Many optical components including modulator, wavelength-division multiplexer and optical switch are required with the rapid development of optical networks. Recently, many research groups have a great deal of interest in the design and fabrication of compact and lightweight optomechanical switches. Optical switches in micro-opto-electromechanical systems (MOEMS) [1–3] have many applications because of their excellent features, such as low insertion loss and crosstalk, wavelength independence and bit-rate transparency [4–6]. Currently, various types of micromechanical switches have been reported in this field [7,8]. Electrostatic actuating is one of the necessary techniques in the fabrication of all kinds of optical switches.

Because of the limit of the dimension of the MOEMS device, the air squeeze film damping is an important factor for most transducers and actuators, such as micromachined microphones, micro-accelerometers, vibratory gyroscopes and micro-optical switches, so the effect of the squeeze film damping on the dynamics of microstructures has been studied [9–11]. Zhang et al. [12] analyzed static characteristics of electrostatic actuating for a torsional micromirror, and Liu et al. [13,14] described the dynamic response using mode-superposition approach. However, the effect of the air squeeze film damping on the devices is not considered in the above reports.

In this paper, a 2 × 2 MOEMS optical switch with electrostatic actuating is presented. Based on the torsion dynamic theory, the method and relative formulae are given for analyzing the actuating voltage and the switching time, on which the effect of the air squeeze film damping is already considered. Furthermore, an optical technique using a linear array CCD is proposed for the measurement of the actuating voltage and the switching time.

2. Structure and performance of the device

The schematic diagram of a 2 × 2 switch is illustrated in Fig. 1, which consists of a micromirror on the cantilever

* Corresponding author. Tel.: +86 431 5168240; fax: +86 431 5168270.
E-mail address: dongmingsun@email.jlu.edu.cn (W.-Y. Chen).

0924-4247/$ – see front matter © 2004 Elsevier B.V. All rights reserved.
doi:10.1016/j.sna.2004.11.033

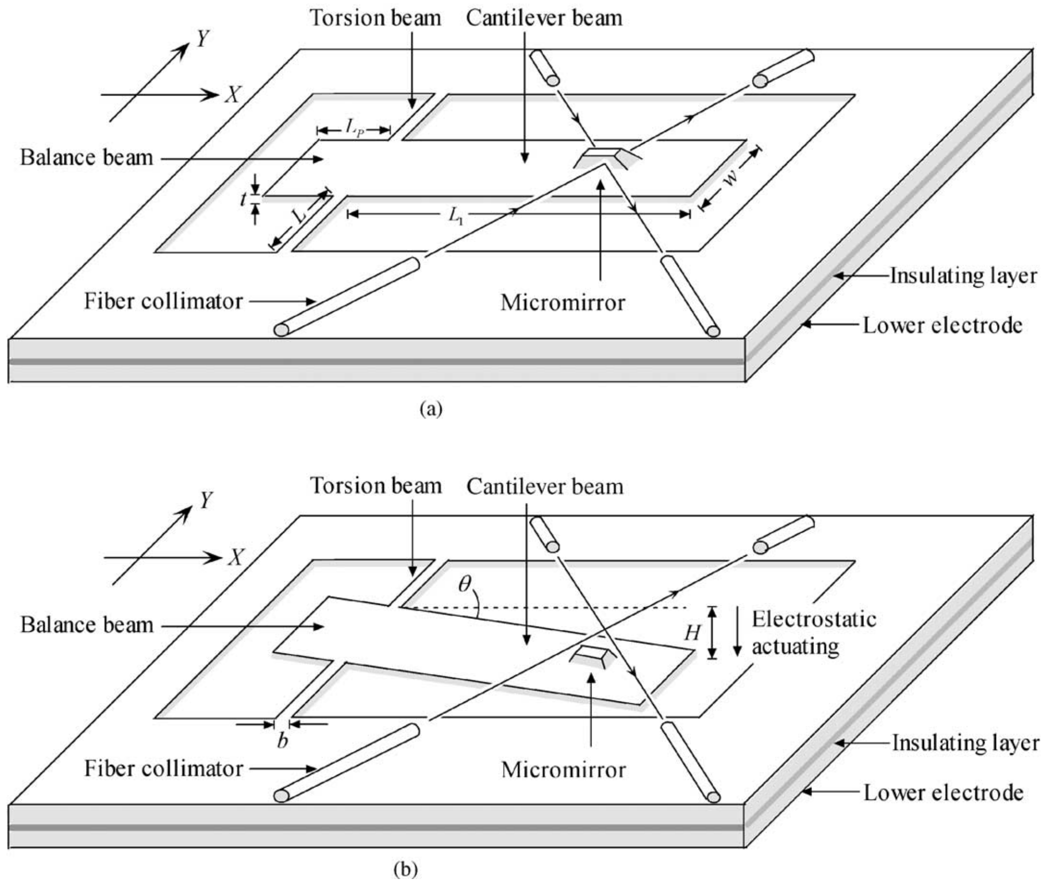

Fig. 1. Sketch diagrams of a 2 × 2 optical switch: (a) reflection state; (b) transmission state.

beam and a lower electrode (i.e. substrate). The micromirror is located in the center of four single-mode fiber collimators placed across. The voltage is applied between the polysilicon cantilever beam and the lower electrode. This voltage creates an electrostatic force that causes a bending angle of the cantilever beam tip. Then the micromirror on the cantilever beam is shifted from the reflection state (Fig. 1a) to the transmission state (Fig. 1b). Consequently, the light from the input waveguide can transmit into the different output waveguides. An air squeeze film is between the cantilever beam and the lower electrode. We define T_{off} as the switching time for conversion of the reflection state into the transmission state, and T_{on} is that for the conversion of the transmission state into the reflection state. The values of some structural parameters are listed in Table 1.

Table 1
Structural parameters of the optical switch

Parameters	Value (unit)
Length of the torsion beam (L) (μm)	700
Width of the torsion beam (b) (μm)	12
Length of the cantilever beam (L_1) (μm)	1900
Width of the cantilever beam (w) (μm)	1000
Thickness of the upper electrode (t) (μm)	10
Length of the balance beam (L_P) (μm)	300
Distance between the upper and lower electrodes (H) (μm)	55

3. Theory of torsion dynamics

3.1. Description of the torque on the cantilever beam

3.1.1. Electrostatic torque

When an actuating voltage V is applied between the cantilever beam and the substrate, an electrostatic force F would occur, of which the expression is as follows [15]:

$$F = \frac{\partial E}{\partial h} = -\frac{\varepsilon_0 s V^2}{2h^2} \tag{1}$$

where E is the electric field intensity, ε_0 the dielectric constant in free space, of which the value is taken to be 8.85×10^{-12} F/M, h the spacing between the upper and lower electrodes, and s the area of the electrode.

The formula of the electrostatic torque M_{E} can be derived as

$$\begin{aligned} M_{\text{E}} &= \frac{\varepsilon_0}{2} V^2 w \int_0^{L_1} \frac{x}{(H/\sin\theta - x)^2 \theta^2} \mathrm{d}x \\ &= \frac{\varepsilon_0 V^2 w}{2\theta^2} \left(\ln \frac{H - L_1 \sin\theta}{H} + \frac{L_1 \sin\theta}{H - L_1 \sin\theta} \right) \end{aligned} \tag{2}$$

where θ is the torsion angle of the cantilever beam.

3.1.2. Restoring torque

The restoring torque M_T of the torsion beam can be expressed as a function of the torsion angle θ [16]:

$$M_T = 2 \times \frac{Gtb^3\theta}{3L}\left[1 - \frac{192}{\pi^5}\frac{b}{t} \cdot \tan h\left(\frac{\pi t}{2b}\right)\right] \quad (3)$$

where G is the shear modulus of polysilicon, of which the value is taken to be 7.3×10^4 MPa [16].

3.1.3. Gravity torque

The cantilever beam would result in a little torsional displacement by the gravity torque, and the balance beam can reduce this displacement. The gravity torque of the cantilever beam M_G and that of the balance beam M_B are given by, respectively

$$M_G = \int_0^{L_1} \rho twgx \cos\theta \, dx = \frac{\rho twg \cos\theta L_1^2}{2} \quad (4)$$

$$M_B = \int_0^{L_P} \rho twgx \cos\theta \, dx = \frac{\rho twg \cos\theta L_P^2}{2} \quad (5)$$

where ρ is the density of polysilicon, and g the acceleration of gravity.

3.1.4. Squeeze film damping torque

The damping is mainly from a small air gap between the cantilever beam and the substrate. The squeeze film damping torque comes from the pressure distribution on the cantilever beam surface. The damping of the air squeeze film can be analyzed by using the following Reynolds' equation [17]:

$$\frac{\partial}{\partial x}\left(h^3\frac{\partial P}{\partial x}\right) + \frac{\partial}{\partial y}\left(h^3\frac{\partial P}{\partial y}\right) = 12\eta\frac{\partial h}{\partial t} \quad (6)$$

where P is the damping pressure caused by the damping of the air squeeze-film, and η the viscosity coefficient of air at room temperature, of which the value is taken to be 1.79×10^{-5} Pa s [17]. By solving Eq. (6), we can obtain the expression of the squeeze film damping coefficient C as (Appendix A):

$$C = \frac{2w\eta}{(2H - L_1\theta)\theta^5} \times \left[L_1\theta(L_1^2\theta^2 - 24H^2 + 6HL_1\theta) + 6H^2(4H - 3L_1\theta)\ln\frac{H}{H - L_1\theta}\right] \quad (7)$$

3.2. Dynamic analysis

According to the dynamic equation of the rigid body [18], we can obtain the following equations of T_{off} and T_{on}, which can determine the values of the angular acceleration β and angular speed ω, as

$$M_E + M_G - M_T - M_B = I\beta + C\omega \quad (8)$$

$$M_T + M_B - M_G = I\beta + C\omega \quad (9)$$

where $C\omega$ is the air squeeze film damping torque, $I = \rho L_1^3 wt/3$ the moment of inertia of the rigid body. The values of T_{off}, T_{on}, β and ω can be solved numerically from Eqs. (8) and (9) (Appendix B). Thus the movement of the cantilever beam is described for every time.

3.3. Calculated results and discussion

Fig. 2 shows the relations between the angular speed ω and the offset of the cantilever beam tip under different actuating voltages. We can see that ω increases with an increase in V. For a certain voltage within 40–55 V, as the offset of the cantilever beam tip increases, first ω increases rapidly, then decreases gradually, and then increases in the second half process of the movement. From the variable tendency of ω, we can conclude that the movement of the cantilever beam is a "destroying balance" but "keeping balance" process. When the actuating voltage is 35 V, the movement of the cantilever beam is a "keeping balance" process. At the point B of the curve, the offset of the cantilever beam tip is about 20 μm, and the value of ω is zero. This indicates that when the actuating voltage is less than 35 V, the cantilever beam moves down incompletely, and stops at the certain location. The cantilever beam keeps balance at this point under the actions of the electrostatic torque, the restoring torque, the gravity torque and the squeeze film damping torque. When the actuating voltage is more than 40 V, the movement of the cantilever beam is a "destroying balance" process. Because of the marked increase of the electrostatic torque, the cantilever beam would continuously move beyond the lowest point A, and would snap down and then stop when the cantilever beam tip touches the lower electrode. This means that the optical switch becomes operational if the actuating voltage is more than 40 V. But different voltages have different effects on the switching time. The switching time would be shorter because of the larger angular speed under the larger actuating voltage.

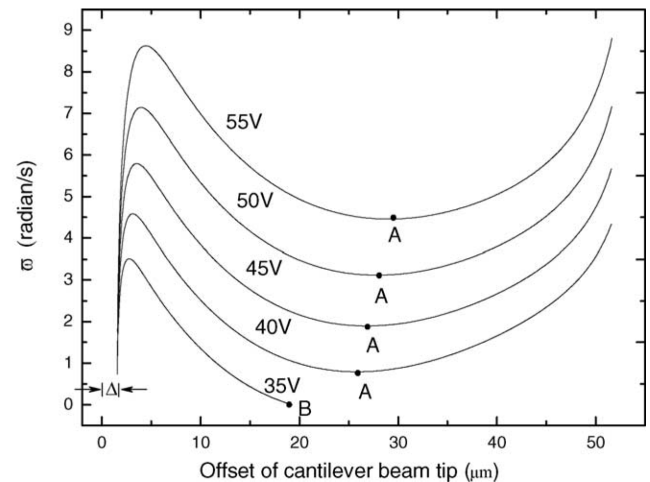

Fig. 2. Relations between the angular speed ω and the offset of the cantilever beam tip.

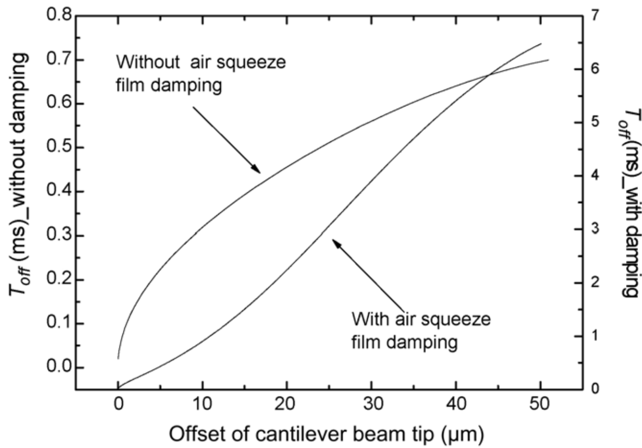

Fig. 3. Effect of the air squeeze film damping on the switching time T_{off}.

The location denoted by symbol Δ shows the initial offset of the cantilever beam tip caused by the gravity torque of the cantilever beam M_G.

The effects of the air squeeze film damping on T_{off} and T_{on} are illustrated in Figs. 3 and 4, respectively, where the actuating voltage is taken to be 50 V. T_{off} or T_{on} is larger greatly when the air squeeze film damping is considered. In Fig. 3 we can see that T_{off} is very different, which is about 0.7 and 6.5 ms for the case of without and with consideration of the air squeeze film damping, respectively. Furthermore, the curve tendency shows that the angular speed ω is not zero because the slope of curve is not zero at the end of movement process. In Fig. 4 we can see that T_{on} is about 0.5 and 15 ms for the case of without and with consideration of the air squeeze film damping, respectively. At the end of movement process, the angular speed ω is approximately equal to zero with consideration of the air squeeze film damping, that is, the cantilever beam would stop at the end of the movement process. This is in good agreement with the actual process. We can conclude from above discussion that the effect of the air squeeze film damping on T_{on} is more obvious than that on T_{off}.

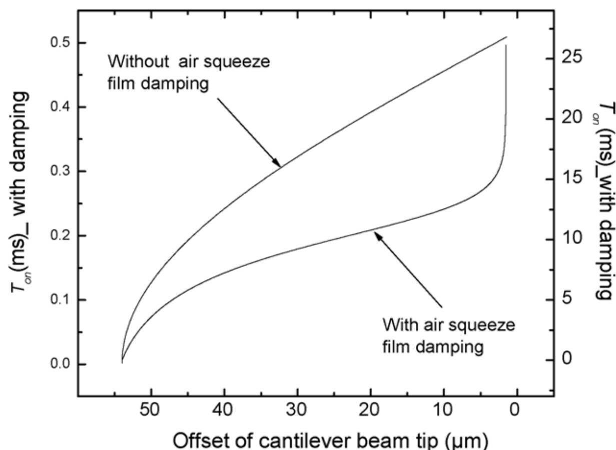

Fig. 4. Effect of the air squeeze film damping on the switching time T_{on}.

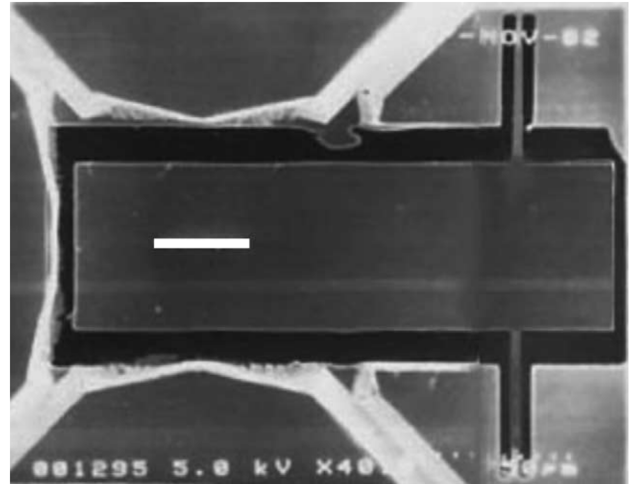

Fig. 5. Diagram showing the monolithic silicon piece, including the V-grooves for optical fibers, the torsion beam, the micromirror and its supporting cantilever beam.

4. Fabrication process

In terms of these optimized structural parameters, this kind of MOEMS optical switch has been fabricated by the processes as follows: (1) LPCVD of silicon nitride (140 nm) on the (1 1 0) silicon wafers as a mask layer for anisotropic etching. (2) Silicon nitride is etched by RIE using the mixture of gases CF_4 and O_2, and the mask of the micromirror and the fiber grooves is obtained. (3) The sample is etched in pure aqueous KOH solution with the concentration of 50 wt.% at 75 °C, then the micromirror and the fiber grooves are formed, at the same time, the thickness of the torsion beams is ensured. (4) The torsion beams and the upper electrode are formed by RIE using the mixture of gases SF_6 and Ar. (5) Al (40 nm) is evaporated on the micromirror. (6) After the metal and the insulation layers of the upper and the lower electrodes are fabricated, the upper and the lower electrode substrates are fixed on the edge. The diagram of the whole silicon part is shown in Fig. 5

5. Measurement method

5.1. Description of the experiment

The experimental set-up is shown in Fig. 6. The light beam from a 5 mW He–Ne laser is focused by some objective lenses and weakened by an attenuator, reflected by both the steering mirror and the cantilever beam in turn, and projected directly onto a CCD camera. The camera is a linear array CCD of 2048 sensors with integral time of 5–300 ms. The dimen-

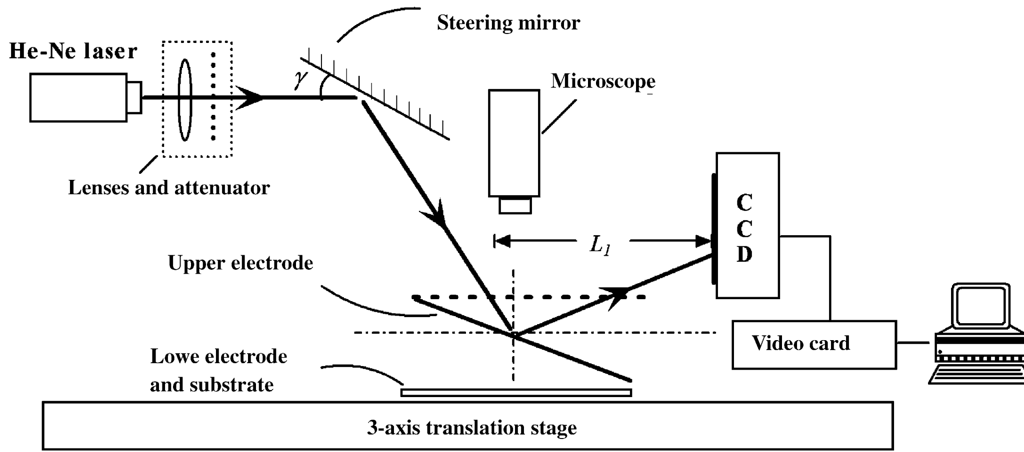

Fig. 6. Sketch map of the experiment equipment.

sion of every sensor is 11 μm × 13 μm, and the distance of adjacent sensors is 13 μm. In order to determine the position of the apparatuses accurately, the optical switch and other equipment are mounted on a three-axis translation stage. The laser beam is directed onto the area on the cantilever beam by careful adjustment of the translation stage. The image captured on the CCD sensors is input into a computer for further processing. By measuring the movement of the laser beam on the screen, the torsion angle of the cantilever beam can be measured.

5.2. Theory analysis

The geometric structural diagram of the beam route is shown in Fig. 7, where θ_1 is the initial torsion angle resulted from the gravity torque, and other parameters are already denoted in the figure. From the geometric relation in Fig. 7, we obtain the equation as follows:

$$\psi = 2\varphi - \tfrac{1}{2}\pi \quad (10)$$

$$\psi + \theta_1 = \tfrac{1}{2}\pi - (\gamma_1 + \theta_1) \quad (11)$$

where ψ is the angle between the vertical and the incident light beam, φ is that between the vertical and the steering mirror, and γ_1 is that between the horizontal and the reflected light beam. The distances of H_1, H_2, ΔH_1 can be expressed as, respectively

$$H_1 = -L_1 \tan(2\theta_1 + 2\varphi) \quad (12)$$

$$H_2 = -L_2 \tan(2\theta + 2\varphi) \quad (13)$$

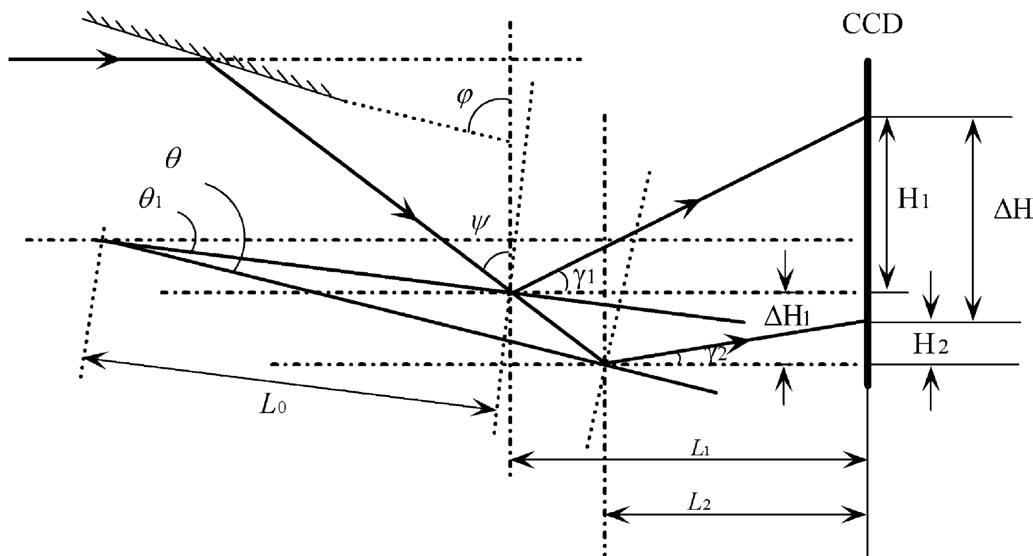

Fig. 7. Geometric structural diagram of the beam route.

$$\Delta H_1 = L_0 \frac{\sin(\theta - \theta_1)\sin(2\varphi)}{\sin(2\varphi + \theta)} \tag{14}$$

where L_0 is the distance between the incident point and the CCD. Finally the distance of ΔH can be derived as

$$\Delta H = \left(L_1 + L_0 \frac{\sin(\theta - \theta_1)\sin(2\varphi)}{\sin(2\varphi + \theta)} \cot(2\varphi) \right) \times \tan(2\theta + 2\varphi) - L_1 \tan(2\theta_1 + 2\varphi) + L_0 \frac{\sin(\theta - \theta_1)\sin(2\varphi)}{\sin(2\varphi + \theta)} \tag{15}$$

Eq. (15) is an implicit function of the torsion angle θ as well as other measurable parameters.

5.3. Results and discussion

The relations between θ and other measurable parameters are discussed by solving Eq. (15). Fig. 8 shows the relations between the angles φ, θ and the distance ΔH. We can see that ΔH increases rapidly with an increase in θ for a sufficient small value of φ, for example $\varphi = 60°$. The measurement method is an "amplification measurement" process, and we should carry on optimization of the values of parameters φ, L_0 and L_1 reasonably.

In the actual experimental, φ, L_0 and L_1 are taken to be 75°, 1500 μm and 15 cm, respectively. The optical signal of the 2048 sensors on CCD is illustrated in Fig. 9. We can obtain the value of the distance ΔH from Fig. 9(a) (without actuating voltage) and (b) (with actuating voltage) to be $\Delta H = (1386 - 446) \times 13\ \mu m = 1.222$ cm. Substituting the values of ΔH and other measurable parameters into Eq. (15), we can calculate the value of the torsion angle θ to be 1.79°. The torsion angle θ is $\sin^{-1}(55/1900) = 1.66°$, so the deviation between them is about 7%. We think that the following two possible reasons lead to most of the deviation besides the observation error. The first is the distance between the cantilever beam and lower electrode. In the assembly process of electrodes, the distance may be increased by the infiltration

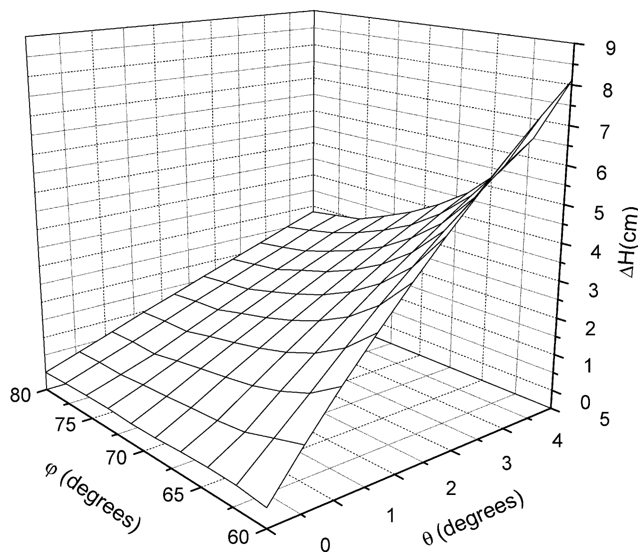

Fig. 8. Relations between the angle of reflector φ, the torsion angle of cantilever beam θ and the distance of the points of incidence on CCD ΔH.

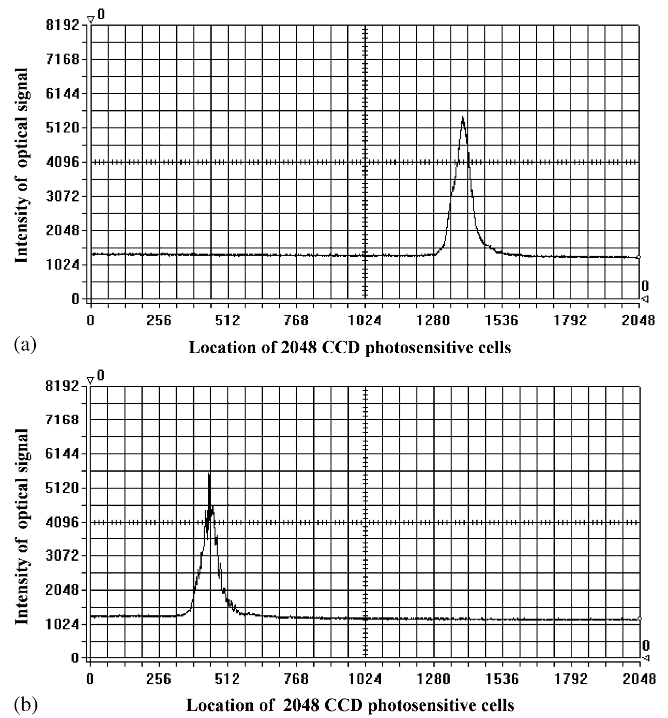

Fig. 9. Drawings of the CCD optical signal (a) without and (b) with the actuating voltage.

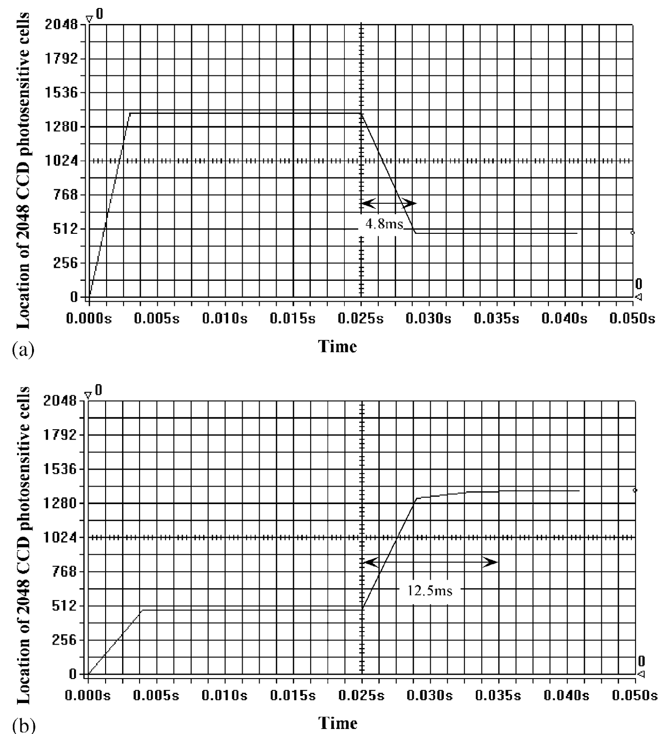

Fig. 10. Drawings of the switching time: (a) T_{off}; (b) T_{on}.

of the gluewater. The second is the deformation of the cantilever beam. When the cantilever beam moves to the lower electrode by the electrostatic force, the cantilever beam may have a deformation by the collision, and the virtual torsion angle would be increased. Therefore, the real torsion angle should be larger than that of the theoretical analysis.

The drawings of the switching time are illustrated in Fig. 10. When the actuating voltage is applied, the cantilever beam moves down, and the location of the optical signal on CCD is changed. We can measure the switching time from the drawings. Fig. 10(a) shows that the switching time T_{off} is 4.8 ms, which is less than the theoretical result (6.5 ms). Fig. 10(b) shows that the switching time T_{on} is 12.5 ms, which is also less than the theoretical result (15 ms). There are many possible reasons lead to the deviation, but the tendency of the measured results is similar to that of the theoretical results.

6. Conclusion

We have demonstrated a 2×2 MOEMS fiber-optical switch with the torsion beam on silicon. The switch is actuated electrostatically and self-assembled. Based on the torsion dynamics theory, the method and relative formulae are presented, and the calculated results are discussed. The switching time is increased greatly when the air squeeze film damping is considered. Therefore, we can draw a conclusion that the air squeeze film damping is an important factor in the study of MOEMS devices. Then an optical method has been proposed for the measurement of the actuating voltage and switching time. The light beams can be captured to further analyze by using a linear array CCD and other optical equipments. The presented set-up and procedures are simpler and more feasible compared some other techniques.

Acknowledgments

The authors wish to express their gratitude to the National Research and Development Plan for High Technology of China (863 Plan) (the project number is 2002AA312023), The National Natural Science Foundation of China (the project number is 69937019) and Jilin Province Science Development Plan (the project number is 20010319) for their generous support of this work.

Appendix A

Because the cantilever beam turns round the torsion beam (y-axis), the distribution of the air pressure P is accordant in the direction of the y-axis, given by

$$\frac{\partial P}{\partial y} = 0 \tag{A.1}$$

The spacing h is expressed as

$$h = H - x\theta \tag{A.2}$$

Substituting Eqs. (A.1) and (A.2) into Eq. (6), we obtain the equation as follows:

$$\frac{\partial^2 P}{\partial x^2} + \frac{3\theta}{x\theta - H}\frac{\partial P}{\partial x} - \frac{12\eta}{(H - x\theta)^3}\frac{\mathrm{d}h}{\mathrm{d}t} = 0 \tag{A.3}$$

Based on the following boundary conditions $x = 0$, $P = 0$ and $x = L_1$, $P = 0$, the damping pressure P can be solved from Eq. (A.3) as

$$P = \frac{12\eta x(x - L_1)}{(2H - L_1\theta)(H - x\theta)^2}\frac{\mathrm{d}h}{\mathrm{d}t} \tag{A.4}$$

The formula of the squeeze film damping torque M_D can be derived as

$$M_D = \int_0^{L_1} \frac{12\eta x(x - L_1)}{(2H - L_1\theta)(H - x\theta)^2}\frac{\mathrm{d}h}{\mathrm{d}t} \cdot x \cdot w \,\mathrm{d}x \tag{A.5}$$

From Eq. (A.2) we have $\mathrm{d}h/\mathrm{d}t = -\dot{\theta}x$, and then substituting it into Eq. (A.5), we finally obtain Eq. (7).

Appendix B

The solution of Eq. (9) is similar to that of Eq. (8), so we only present the solution of Eq. (8) as follows. If we define $M(\theta) = M_E + M_G - M_T - M_B$, Eq. (8) can be written as

$$M(\theta) = I\beta + C\omega \tag{B.1}$$

We divide the switching time T into n increments, each of them is $\Delta T = T/n$. Denote torsion angle as θ_i at the ith point, then ω_i and β_i can be written as

$$\omega_i = \dot{\theta}_i = \frac{\theta_{i+1} - \theta_{i-1}}{2\Delta T} \tag{B.2}$$

$$\beta_i = \ddot{\theta}_i = \frac{\theta_{i+1} - 2\theta_i + \theta_{i-1}}{\Delta T^2} \tag{B.3}$$

Substituting Eqs. (B.2) and (B.3) into Eq. (B.1), we can obtain the iterative formula as follows:

$$\theta_{i+1} = \frac{[2I\theta_i + ((C(\theta_i)\Delta T/2) - I)\theta_{i-1} + M(\theta_i)\Delta T^2]}{I + (C(\theta_i)\Delta T/2)} \tag{B.4}$$

where $C(\theta_i)$ and $M(\theta_i)$ are functions of θ. By using the initial conditions $\theta_0 = 0$ and setting the value of ΔT, then θ_i can be calculated from Eq. (8). According to Eq. (B.4), we can obtain the value of θ for every time step. The values of T_{off}, T_{on}, β and ω can be calculated by the iterative process.

References

[1] M.N. Horenstein, S. Pappas, A. Fishov, T.G. Bifano, Electrostatic micromirrors for subaperturing in an adaptive optics system, J. Electrostat. 54 (2002) 321–332.

[2] M. Hoffmann, E. Voges, Bulk silicon micromachining for MEMS in optical communication systems, J. Micromech. Microeng. 12 (2001) 349–360.
[3] B. McCarthy, V.M. Bright, J.A. Neff, A multi-component solder self-assembled micromirror, Sens. Actuators A 103 (2003) 187–193.
[4] C. Marxer, C. Thio, M.A. Gretillat, N.F. de Rooij, R. Batting, O. Anthamatten, B. Valk, P. Vogel, Vertical mirrors fabricated by deep reactive ion etching for fiber-optic switching applications, J. Microelectromech. Syst. 6 (1997) 227–285.
[5] M. Hill, C. O'Mahony, H. Berney, P.J. Hughes, E. Hynes, W.A. Lane, Verification of 2-D MEMS model using optical profiling techniques, Opt. Lasers Eng. 36 (2001) 169–183.
[6] L.Y. Lin, E.L. Goldstein, R.W. Tkach, On the expandability of free-space micromachined optical cross-connects, J. Lightw. Technol. 18 (2000) 482–489.
[7] J.M. Huang, A.Q. Liu, C. Lu, J. Ahn, Mechanical characterization of micromachined capacitive switches: design consideration and experimental verification, Sens. Actuators A 108 (2003) 36–48.
[8] W. Dong, S.P. Ruan, X.D. Zhang, C.X. Liu, D.M. Sun, C.P. Jia, J.X. Pan, P. Ji, W.Y. Chen, Design and fabrication of slant-counter electrodes for optical switches, Microwave Opt. Technol. Lett. 41 (4) (2004) 273–275.
[9] J.B. Starr, Squeeze-film damping in solid-state accelerometers, Technical Digest, in: Proceedings of the IEEE Solid-state Sensors and Actuators Workshop, 1990, pp. 44–47.
[10] M. Andrews, I. Harris, G. Turner, A comparison of squeeze-film theory with measurements on a microstructure, Sens. Actuators A 36 (1993) 79–87.
[11] Y.J. Yang, S.D. Senturia, Numerical simulation of compressible squeeze-film damping, Technical Digest, in: Proceedings of the Solid-state Sensors and Actuators Workshop, 1996, pp. 76–79.
[12] X.M. Zhang, F.S. Chau, C. Quan, Y.L. Lam, A.Q. Liu, A study of the static characteristics of a torsional micromirror, Sens. Actuators A 90 (2001) 73–81.
[13] A.Q. Liu, X.M. Zhang, V.M. Murukeshan, Q.X. Zhang, Q.B. Zou, S. Uppili, Optical switch using draw-bridge micromirror for large array crossconnects, in: Proceedings of the 11th International Conference on Solid-state Sensors and Actuators, Transducer'01, Eurosensors XV, Munich, Germany, June 10–14, 2001, pp. 1324–1327.
[14] A.Q. Liu, X.M. Zhang, C. Lu, F. Wang, C. Lu, Z.S. Liu, Optical and mechanical models for a variable optical attenuator using a micromirror drawbridge, J. Micromech. Microeng. 13 (3) (2003) 400–411.
[15] H. Toshiyoshi, H. Fujita, Electrostatic micro-torsion mirrors for an optical switch matrix, J. Microelectromech. Syst. 5 (4) (1996) 231–237.
[16] S.S. Lee, L.S. Huang, C.J. Kim, M.C. Wu, Free-space fiber-optic switches based on MEMS vertical torsion mirrors, J. Lightw. Technol. 17 (1999) 7–13.
[17] F. Pan, J. Kubby, E. Peeters, A.T. Tran, S. Mukherjee, Squeeze film damping effect on the dynamic response of a MEMS torsion mirror, J. Micromech. Microeng. 8 (1998) 200–208.
[18] T.W.B. Kibble, Classical Mechanics, 2nd ed., McGraw-Hill, London, 1973, Chapter 10.

Biographies

Dong-Ming Sun received his BSc and MSc degrees in Microelectronics and Solid Electronics from the College of Electronic Science and Engineering, Jilin University, Changchun, China, in 2001 and 2003, respectively, where he is currently working toward his PhD degree. His research interests include design and fabrication of MOEMS optical switch.

Wei Dong received her BSc and MSc degrees from the College of Mechanical Electronics, Harbin Institute of Technology, Harbin, China, in 1996 and 1998, respectively. And she received her DSc degree in Microelectronics and Solid Electronics from the College of Electronic Science and Engineering, Jilin University, Changchun, China, in 2004. Her research interests include design and fabrication of MOEMS devices.

Guo-Dong Wang received his BSc and MSc degrees in Microelectronics and Solid Electronics from the College of Electronic Science and Engineering, Jilin University, Changchun, China, in 2001 and 2003, respectively, where he is currently working toward his PhD degree. His research interests include design and fabrication of fiber grating.

Cai-Xia Liu is currently an engineer in the College of Electronic Science and Engineering and the State Key Laboratory on Integrated Optoelectronics, Jilin University, Changchun, China. Her main areas of research are design and fabrication of optoelectronic devices.

Xin Yan received her BSc and MSc degrees in Microelectronics and Solid Electronics from the College of Electronic Science and Engineering, Jilin University, Changchun, China, in 2001 and 2003, respectively, where she is currently working toward her PhD degree. Her research interests include guided-wave optics and integrated optoelectronics. Currently she is devoting to the computer-aided design and technological process of the arrayed waveguide grating (AWG) and microring resonator (MRR) devices.

Bao-Kun Xu is currently a professor in the College of Electronic Science and Engineering and the State Key Laboratory on Integrated Optoelectronics, Jilin University, Changchun, China. His main areas of research are design and fabrication of optoelectronic devices.

Wei-You Chen received his BSc, MSc and DSc degrees in Optoelectronics from the Department of Electronic Engineering, Jilin University, Changchun, China, in 1986, 1989 and 1992, respectively, where he is currently a Professor in the College of Electronic Science and Engineering and the State Key Laboratory on Integrated Optoelectronics. His main areas of research are guided-wave optics, nonlinear optics and integrated optoelectronics, and his interests include the characteristic analysis, computer-aided design and fabrication of optoelectronic devices.